



OPEN

Protecting playgrounds: local-scale reduction of airborne particulate matter concentrations through particulate deposition on roadside 'tredges' (green infrastructure)

Barbara A. Maher¹✉, Tomasz Gonet^{1,4}, Vassil V. Karloukovski¹, Huixia Wang² & Thomas J. Bannan³

Exposure to traffic-related particulate air pollution has been linked with excess risks for a range of cardiovascular, respiratory and neurological health outcomes; risks likely to be exacerbated in young children attending schools adjacent to highly-trafficked roads. One immediate way of reducing airborne PM concentrations at the local (i.e., near-road community) scale is installation of roadside vegetation as a means of passive pollution abatement. Roadside vegetation can decrease airborne PM concentrations, through PM deposition on leaves, but can also increase them, by impeding airflow and PM dispersion. Critical to optimizing PM removal is selection of species with high particle deposition velocity (V_d) values, currently under-parameterised in most modelling studies. Here, the measured amounts of leaf-deposited magnetic PM after roadside greening ('tredge') installation, and measured reductions in playground PM, particle number and black carbon concentrations demonstrate that air quality improvements by deposition can be achieved at the local, near-road, community/playground scale. PM deposition on the western red cedar tredge removed ~49% of BC, and ~46% and 26% of the traffic-sourced $PM_{2.5}$ and PM_{10} , respectively. These findings demonstrate that roadside vegetation can be designed, installed and maintained to achieve rapid, significant, cost-effective improvement of air quality by optimising PM deposition on plant leaves.

Exposure to the traffic-related air pollution (TRAP) associated with proximity to major roads has been linked with excess risks for a range of cardiovascular and respiratory health outcomes. Air pollution comprises a mix of gases and solid particles of varying sizes. Exposure to fine particulate matter ($PM_{2.5}$, < 2.5 μm in aerodynamic diameter) in air pollution is reportedly the largest environmental risk factor contributing to cardiovascular mortality and morbidity, globally¹⁻³, and causes about six to nine million premature deaths each year^{4,5}.

Evidence increasingly shows that exposure to airborne PM is also linked with impaired neuro-development and cognitive function. Robust correlations have been found between outdoor PM concentrations and reduced brain function, in different geographic settings and age groups. Epidemiological studies have shown measurable neurological impacts at PM concentrations below current policy limits/recommendations (e.g.^{6,7}).

Infants and young children are particularly vulnerable to the impacts of air pollution, incurring health burdens blighting their entire life span. Their major organs are still undergoing development. They inhale higher PM doses given their lower lung volume and higher breathing rate (double that of an adult per unit of body weight)⁸. As pedestrians, they are closer in height to peak concentration height (~0.3 m) of vehicle-derived PM⁹. While residential proximity to major roads has been associated with adverse health outcomes (e.g.^{10,11}), school location

¹Centre for Environmental Magnetism and Palaeomagnetism, Lancaster Environment Centre, Lancaster University, Lancaster LA1 4YQ, UK. ²School of Environmental and Municipal Engineering, Xi'an University of Architecture and Technology, Xi'an 710055, Shaanxi, People's Republic of China. ³School of Earth, Environmental and Atmospheric Science, University of Manchester, Manchester, UK. ⁴Present address: Jaguar Land Rover, Gaydon, Lighthorne Heath, Warwick CV35 0BJ, UK. ✉email: b.maher@lancaster.ac.uk

may also be an important determinant of children's exposure to traffic-related pollutants^{12,13}. Internationally, millions of children are exposed to elevated TRAP levels by attending schools located close to major roads, especially those attending schools in low-income neighbourhoods (e.g.^{14–16}). Children attending schools in areas with high levels of particulate air pollution displayed deficits in cognitive development in Barcelona, Spain^{17,18}. Other epidemiological studies indicate cognitive deficits in young people exposed to high TRAP concentrations (e.g.^{19,20}). Long-term PM_{2.5} exposure has been linked with behavioural problems; e.g., increased delinquency of urban-dwelling adolescents in Southern California, USA²¹. Airborne PM is also linked with incidence of premature birth and low birth weight^{22,23}, and mortality in paediatric, adolescent and young adult patients with specific cancers²⁴. Exposure to carbonaceous TRAP is associated with increased all-cause, neurodegenerative and cardiovascular mortality risks (25–27).

Globally, road traffic constitutes the largest (albeit declining²⁸) single source of outdoor air pollution in urban environments²⁹. Vehicles and associated road wear produce airborne PM very effectively, from a range of sources, and with a range of particle sizes and compositions. Gases, such as nitrogen dioxide, are emitted from exhausts, as are semi-volatile and solid particles, often a mixture of carbon and various bioreactive metal species (including iron, manganese, nickel, chromium, lead, platinum). Solid particles are produced abundantly from wear of brakes, tyres, and road surfaces³⁰ as well as exhausts. Those produced by brake wear are often ultrafine in size (< 100 nanometers, nm) and rich in iron, including metallic and magnetic forms of iron, such as magnetite^{31–33}. Hence, magnetic measurements of airborne PM often demonstrate strong direct correlation with more conventional measurements of PM and NO_x, for example^{34–36}.

The causal role of airborne PM in driving adverse health outcomes in children is attested independently by observed mitigation of health impacts after reducing outdoor PM concentrations. Critically, even small improvements in air quality result in measurably improved health outcomes. In East Germany, the decline of coal combustion-related air pollution after reunification was associated with improved lung function in children³⁷. Within a cohort of children in California, those who moved to areas with lower levels of PM₁₀ (< 10 µm aerodynamic diameter) showed increased lung function growth; those who moved to more polluted areas experienced decreased lung function growth³⁸.

Given the health impacts of TRAP, especially for young children, policy-driven reduction of PM emissions is essential and urgent but in practice is slow and incremental. One immediate and practical way of reducing airborne PM concentrations at the local (i.e., near-road community) scale may be the installation of green infrastructure, such as roadside trees/shrubs/hedges/grasses (e.g.^{9,39–42}). This role for roadside vegetation as a means of passive pollution abatement (combined with other ecosystem services) is increasingly recognised globally. A fast-growing body of published papers has reported a remarkably large range of experimental (real-world) and modelled outcomes of the effects of roadside greening on PM levels. A recent review by the Nature Conservancy⁴³ collates much of this disparate evidence.

Critically, roadside vegetation can decrease airborne PM concentrations, through PM deposition on leaves, but can also lead to increased PM concentrations, by impeding airflow and altering PM dispersion. The 'competition' between these two mechanisms determines the air quality at pedestrian/road user level, and the amount of PM leaving the road area/vegetation canopy⁴⁴.

Recent modelling-based papers and expert reviews (e.g.⁴⁵) state that the magnitude of PM *deposition* on urban vegetation is small in most street contexts; 'dwarfed'⁴⁶ by the effects that street vegetation has on *dispersion* of local PM. Such studies mostly use computational fluid dynamics (CFD) to simulate PM emission, dispersion and deposition, and, typically, indicate small reductions (i.e., a few percent) in PM₁₀ or PM_{2.5} concentrations by deposition onto (mostly existing, often very tall) roadside vegetation (e.g.^{47–50}). Common to most of these studies is their standardised parameterisation of a critical factor, the velocity of particle deposition to leaf surfaces.

The deposition velocity (V_d) is the quotient of the particle mass flow rate (F_p , in µg m⁻² s⁻¹) towards the leaf surface and the atmospheric particle concentration (C_p , in µg m⁻³), normally given in m s⁻¹ or cm s⁻¹:

$$V_d = F_p/C_p$$

V_d varies with many factors, including particle size and density, surface morphology, meteorological conditions (wind speed, humidity, rainfall, atmospheric stability), ambient concentrations of other (e.g. gaseous/semi-volatile) pollutants. Such multifactorial, often stochastic variability in V_d may account for the diverse reported PM removal rates by vegetation. However, V_d also varies markedly with plant species (and sub-species/cultivar), via leaf surface traits, leaf size, morphology and number, canopy structure (e.g.^{35,41,51–55}), and as yet poorly known physicochemical interactions between leaves and airborne particles, and between particles (especially for sub-micrometre PM).

The *modelled* effectiveness of PM removal by vegetation depends substantively on the V_d value selected for the model^{41,44,56–58}. The 'standard' V_d values used in most modelling studies of PM deposition vs dispersion effects are typically 0.64 cm s⁻¹ or 0.1 cm s⁻¹ for PM_{2.5} (e.g.^{48,49,59}) and 0.2 cm s⁻¹ for PM₁₀ (e.g.⁵⁰).

Self-evident is that modelled estimates of PM removal by deposition will be low when the 'standard' V_d value used in those models is low (i.e., ~ 0.1 to 0.64 cm s⁻¹). If the selected V_d is unrealistically low, then such studies may misrepresent the potential efficacy of roadside greening, especially at the local, near-road community/playground scale, and in the context of new roadside greening schemes, where high- V_d species can be selected explicitly (e.g.^{41,58}).

The species-dependence of V_d (e.g.^{35,60–62}) appears of key and currently overlooked importance in optimising roadside greening. ('Plant species' hereafter also refers to sub-species and cultivar). Using magnetic particle loadings as a proxy for PM₁₀, Mitchell et al.³⁵ reported (magnetic) species-specific V_d values, varying as a function of leaf micro-topography, especially hairiness and rugosity (i.e., small-scale variations in leaf surface height/topography); as subsequently attested, for a diverse species range, by e.g.⁶³. Lowest V_d values (0.5 to 0.9 cm s⁻¹)

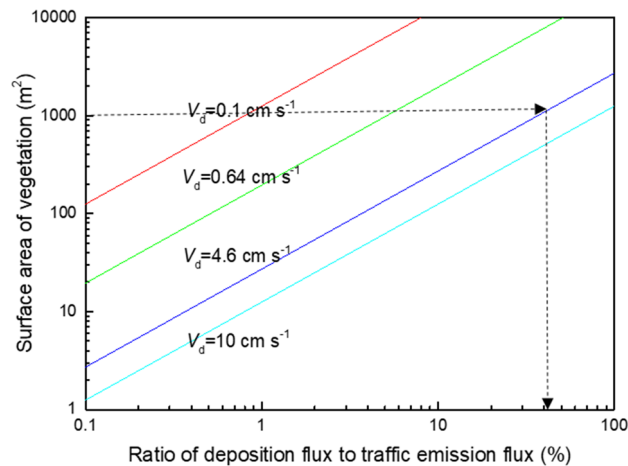


Figure 1. Ratio of vegetation deposition flux to traffic emission flux; depending on surface area of vegetation with differing leaf deposition velocity (V_d) in a street canyon of 100 m length with annual PM_{10} concentration of $37 \mu\text{g m}^{-3}$, average emission factor $100 \mu\text{g vehicle}^{-1} \text{m}^{-1}$ for PM_{10} , traffic intensity of $\sim 40,000$ vehicles day^{-1} (adapted from^{56,58}). The black dashed lines indicate the % PM_{10} removal ($\sim 40\%$) by leaf deposition, with 8 silver birch trees ($V_d = 4.6 \text{ cm s}^{-1}$, canopy diameter 8 m, total leaf surface area = $125 \text{ m}^2/\text{tree}$).

were measured for sweet chestnut, elder, elm, and willow (similar, long term average values, 0.7 to 1.07 cm s^{-1} , were reported for mixed stands of sweet chestnut, oak, holly, yew and Scots pine⁶⁴). Mitchell et al.³⁵ reported intermediate values (~ 1.3 to 1.9 cm s^{-1}) for sycamore, horse chestnut, ash, and maple; and higher V_d values (2.4 to 4.6 cm s^{-1}) for lime, beech, and silver birch (particles agglomerating in extremely high numbers for birch within leaf surface micro-furrows, SI Fig. S1). Even higher V_d values (for $PM_{1-PM_{10}}$), $> 8 \text{ cm s}^{-1}$, have been reported for grassland⁶⁵ and Douglas fir⁵³, dependent on/increasing with wind speed⁵².

The significance of leaf V_d parameterisation for estimating depositional removal of local, traffic-derived PM is demonstrated in Fig. 1. Taking, for example, our experimentally-derived V_d of 4.6 cm s^{-1} (silver birch, Mitchell et al., 2010) with leaf surface area of $125 \text{ m}^2/\text{tree}$ (canopy diameter 8 m), 8 silver birch trees/100 m street length would remove $\sim 40\%$ of the traffic-derived PM_{10} (Fig. 1). Such removal rates appear congruent with indoor PM measurement campaigns for roadside birch⁴¹ and other green structures ('hedge', 'tree', species not identified) as summarised by^{39,66}.

Conversely, if a conventional, 'standard' V_d value of 0.1 or 0.64 cm s^{-1} is assumed (Fig. 1), then the estimated PM removal by those eight trees would be just ~ 1 to 5% of the traffic-emitted PM_{10} . Using the low 'standard' V_d values, an unfeasibly large number of trees (> 80 trees/100 m road) would be needed, to provide the enormous surface area necessary to compensate for the low assumed V_d , and thence increase the estimated PM removal to any significant portion of the local, traffic-emitted PM_{10} .

Apparent then from Fig. 1 is that local-scale planting of species selected for their *high* V_d (i.e., $> \sim 2 \text{ cm s}^{-1}$), sited close to the local, traffic-related PM sources, could substantively reduce local PM concentrations through leaf deposition. Here, we installed different types of 'tredges' (i.e., trees managed as hedges) along the existing wire fences separating three primary school playgrounds from major arterial (non-canyon) roads in Air Quality Management Areas in Manchester, UK, to investigate their efficacy in reducing playground PM, particle number concentrations (PNC) and black carbon (BC).

Air quality and leaf magnetic measurements indicate greatest playground PM reductions (probably by airflow blocking) by the ivy screen ($\sim 25\%$ for median $PM_{2.5}$ and PM_1 , 14% for PNC, no reduction in BC), and greatest playground PM reductions (by leaf deposition) by the evergreen western red cedar tredge ($\sim 23\%$ for median $PM_{2.5}$, 13% for PM_1 , 16% for PNC, 49% for BC). The incidence of short-lived, high-magnitude peaks in PM and PNC was substantially reduced; for example, by 67–82% for $PM_{2.5}$, PM_1 and PNC behind the western red cedar tredge. These findings highlight that local-scale planting campaigns of high- V_d roadside tredges can contribute immediately to mitigation of health hazard, especially where particularly vulnerable population groups (e.g. young children) are exposed to PM from proximal, heavily-trafficked roads.

Results

PM concentrations. Figure 2 shows the PM_{10} concentrations (hourly means) at the roadside and distal playground (7 to 15 m from roadside) for the four schools (SI Fig. S2), over the monitored summer/autumn interval (June to October 2019, Cambri sensor network; data summaries in SI Figs. S3–14), together with vehicle count data (2019) for each location. SI Figs. S3 and S4 show the $PM_{2.5}$ and PM_1 concentrations for the same interval. Monthly roadside PM levels were highest in August/September and lowest in July (SI Table S1).

The least heavily-trafficked school location, Abbott, experienced the highest levels (averaged over the 5-month measurement period) of PM_{10} ($\sim 10.4 \mu\text{g}/\text{m}^3$) and $PM_{2.5}$ ($\sim 6.4 \mu\text{g}/\text{m}^3$), compared to $8.8 \mu\text{g}/\text{m}^3$ (PM_{10}) and $6.3 \mu\text{g}/\text{m}^3$ ($PM_{2.5}$) for Medlock, $8.3 \mu\text{g}/\text{m}^3$ (PM_{10}) and $6.1 \mu\text{g}/\text{m}^3$ ($PM_{2.5}$) for St Ambrose, and $8.0 \mu\text{g}/\text{m}^3$ (PM_{10}) and $6.2 \mu\text{g}/\text{m}^3$ ($PM_{2.5}$) for MCA. Similar levels of PM_1 were noted for all the schools, $\sim 3.1 \mu\text{g}/\text{m}^3$ at Medlock, Abbott

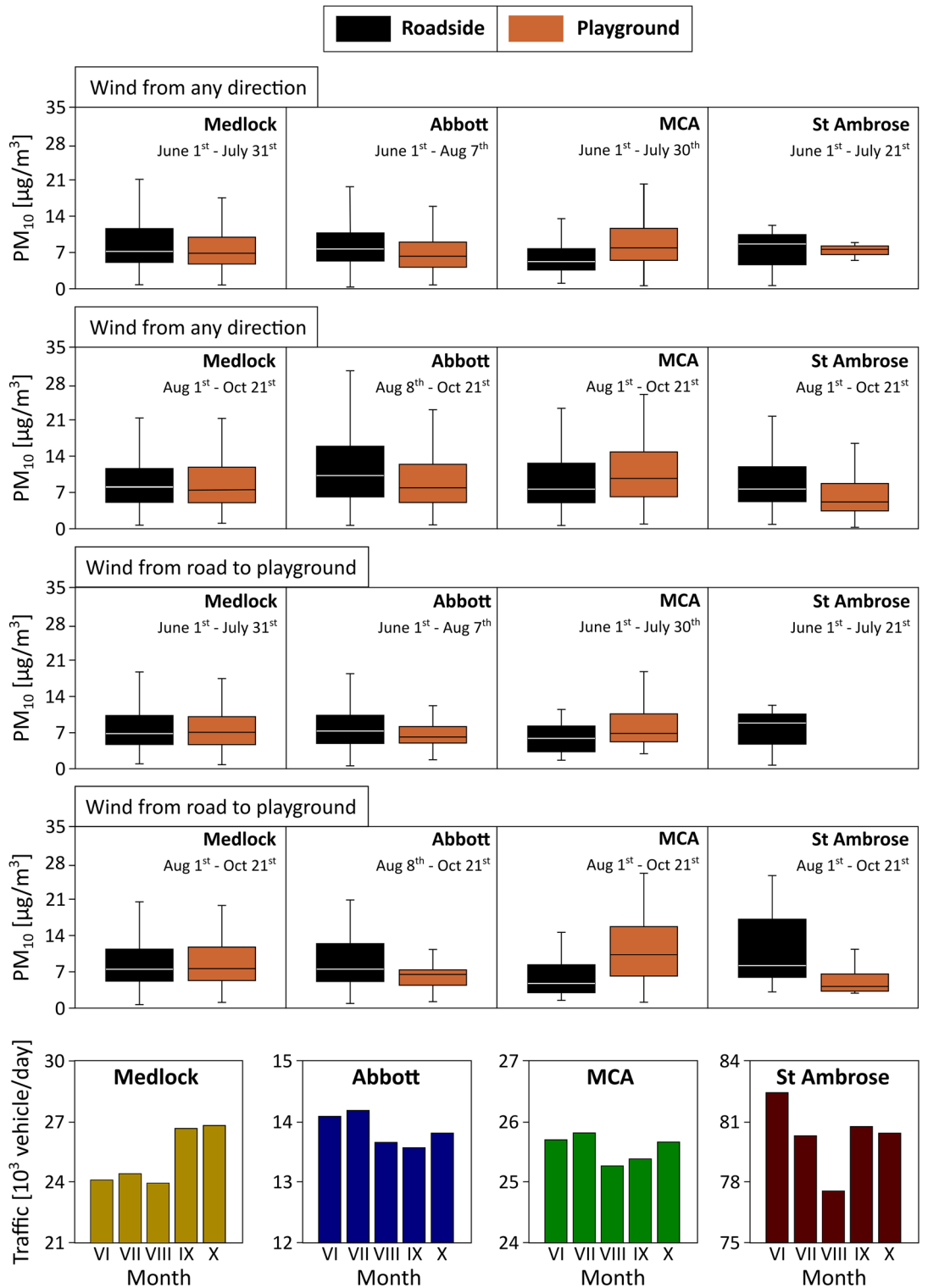


Figure 2. PM₁₀ concentrations (hourly average) for summer (pre-tredden installations) and late summer/autumn, 2019 at the roadside and at distal playground (14–17 m from roadside for Medlock, Abbott and St Ambrose, 7 m for MCA), and the road traffic volume for the 4 schools. In the box-whisker plots, boxes indicate median value, lower and upper quartiles, and whiskers show 10th and 90th percentiles. The absence of data (St Ambrose summer) reflects sensor malfunction.

and MCA, and ~2.9 µg/m³ at St Ambrose. Co-location of a Cambri sensor at the University of Manchester air quality supersite indicates these measured PM₁₀, PM_{2.5}, and PM₁ concentrations are lower, on average, by ~36%,

15% and 69%, respectively, than those recorded by a certificated aerosol spectrometer (Palas FIDAS 200 E). The FIDAS, in turn, was calibrated according to the UK MCERTS specification for particulate matter, and audited by the UK National Physical Laboratory.

The measured $PM_{2.5}$ concentrations exceeded the WHO's (2021) recommended annual mean limit ($5 \mu\text{g}/\text{m}^3$) for all schools. For PM_{10} , the measured average levels were within the current recommended limit (annual mean $15 \mu\text{g}/\text{m}^3$) for all schools. Notable, however, is the very high temporal variability of PM at each school, reaching high but short-lived peaks (up to even $16 \times$ higher than the average values). For example, the highest PM_{10} value (hourly average) was observed at MCA on July 24th 2019 ($74.2 \mu\text{g}/\text{m}^3$), and highest $PM_{2.5}$ ($64.2 \mu\text{g}/\text{m}^3$) at MCA on September 22nd 2019, and PM_1 ($50.2 \mu\text{g}/\text{m}^3$) at MCA on July 24th 2019.

PM concentrations—roadside and playground. Tredges were installed at three of the schools during the school holidays (July/August 2019). An ivy screen was installed at Abbott School; western red cedar at St Ambrose School; a roadside trede of alternating western red cedar/Swedish birch and an inner juniper hedge at MCA. Medlock, the 'control' school (i.e., no trede installation), demonstrates negligible distance decay effect in roadside vs playground PM concentrations throughout the monitored interval (Fig. 2). Abbott and St Ambrose schools similarly display little roadside/playground differences in PM concentrations in the summer period, prior to trede installation. (The 'playground' sensor at MCA was affected by an air conditioning exhaust outlet, and recorded consistently increased PM values compared with roadside; hence, omitted from further consideration here). After trede installation, Abbott (ivy screen) displays a small reduction in playground PM concentrations, while St Ambrose (western red cedar) displays a larger PM reduction (Fig. 2; SI Figs. S3 and S4). These playground PM reductions were greater when the wind direction was from the road to the playground (Fig. 2; SI Figs. S3 and S4). The significance of these measured roadside/playground PM reductions is uncertain, however, given the estimated between-sensor uncertainties (which range from 22 to 31% for PM_{10} , 10–15% for $PM_{2.5}$, and 9–14% for PM_1 , SI Table S2).

Hence, additional air quality measurements were made (Fig. 3). Black carbon (BC) was measured simultaneously at roadside and playground, at the three schools with tredges, in November 2020, and $PM_{2.5}$, PM_1 , and particle number concentrations (PNCs) measured (portable optical particle spectrometers, POPS) simultaneously at the roadsides, and in the playgrounds at 1 m and ~ 5 m behind the tredges in April 2021, after further growth of the tredges. Between-sensor uncertainty estimates for the BC measurements range from 2 to 12%, and for the POPS measurements from 1 to 6% (SI Table S3).

BC values are significantly ($\sim 5 \times$) higher for the most heavily-trafficked site, St Ambrose (Fig. 3) (t-test; $p < 0.05$). The high and variable PM concentrations but lower BC (and NO, SI Fig. S11) values measured at Abbott may reflect emissions from non-road traffic sources; a 6-track railway line lies ~ 100 m to the west (SI Fig. S2). Bivariate polar plots indicate high PM concentrations at Abbott are associated with moderate westerly winds (SI Fig. S14).

$PM_{2.5}$ and PM_1 concentrations, measured by the POPS instruments, are in good agreement with those from the Cambri sensors (Figs. 2, 3; SI Figs. S3–10). For the roadside sensors, PNCs were highest for St Ambrose (median $\sim 9877 \text{ \#/cm}^3$), followed by Abbott ($\sim 5545 \text{ \#/cm}^3$), and MCA (5234 \#/cm^3) (Fig. 3; SI Table S3). At all three schools, measurable (and statistically significant; $p < 0.05$) reductions in $PM_{2.5}$, PM_1 , and PNC were observed in the playgrounds (Fig. 3; Table S3). The measurements indicate greatest playground PM reductions by the ivy screen; $\sim 25\%$ for median $PM_{2.5}$ and PM_1 , 14% for PNC, but 5% increase in black carbon (BC). Behind the evergreen western red cedar trede at St Ambrose, the playground reductions were 23% for median $PM_{2.5}$, 13% for PM_1 , 16% for PNC, and 49% for BC. Moreover, the tredges substantially reduced the magnitude and frequency of acute 'spikes' in PM and BC concentrations; for example, by 67–82% for $PM_{2.5}$, PM_1 and PNC in the St Ambrose playground (SI Table S3). At MCA, behind the outer trede (alternating western red cedar/Swedish birch) and inner row of juniper, the playground reductions are lower; 9%, 6%, 11% and 16% for $PM_{2.5}$, PM_1 , PNC and BC, respectively (SI Table S3).

Leaf magnetic loadings and PM deposition estimates. 'Clean' leaves should display negligible magnetic remanence, because of their high content of carbon and water (which display diamagnetic behaviour, i.e., negative magnetic susceptibility, zero magnetic remanence). However, traffic-derived PM always contains strongly magnetic particles, produced especially by brakewear^{31,67}, vehicle exhausts, tyrewear etc. Deposition of magnetic PM on leaves makes them variably magnetic⁶⁸. The amount of magnetic PM deposited on our tredges was quantified by measuring the saturation remanent magnetisation (SIRM) of leaf samples from the roadside and playground sides of the tredges (Fig. 4). Western red cedar leaves (St Ambrose, and MCA) collected the greatest amounts of magnetic grains, as measured by SIRM ranging between 98×10^{-6} A and 159×10^{-6} A (roadside). For these cedar tredges, the roadside SIRM values were 2–5 \times higher than the playground side (Fig. 4). Much lower SIRM values were obtained for the ivy leaves at Abbott (18×10^{-6} A roadside) and the inner juniper trede at MCA (41×10^{-6} A roadside), and no decrease in leaf SIRM was observed from the roadside to the playground side for these species (Fig. 4).

We also measured another type of magnetic remanence, anhysteretic remanent magnetisation (ARM), which is sensitive to magnetic particles ~ 25 nm in size. As with SIRM, highest χ_{ARM} values were obtained for western red cedar at St Ambrose ($17\text{--}34 \times 10^{-9}$ m) and MCA (28×10^{-9} m), with significant decrease ($\times 2\text{--}4$) for the playground sides (Fig. 4). The ivy at Abbott and juniper at MCA collected much lower amounts of ultrafine magnetic grains (χ_{ARM} from 4 to 7×10^{-9} m), with no reductions from the roadside to the playground sides. PM deposition on ivy leaves has been reported^{69,70} to be lower (e.g., 8–14 $\mu\text{g}/\text{cm}^2$; up to 30 $\mu\text{g}/\text{cm}^2$ ⁶¹) than numerous other broadleaved and coniferous species, which display leaf PM loadings of $> 50\text{--}230 \mu\text{g}/\text{cm}^2$ (e.g.^{61,71}). While the SIRM and χ_{ARM} values varied for the leaves at the three schools, the SIRM/ χ_{ARM} ratio was relatively

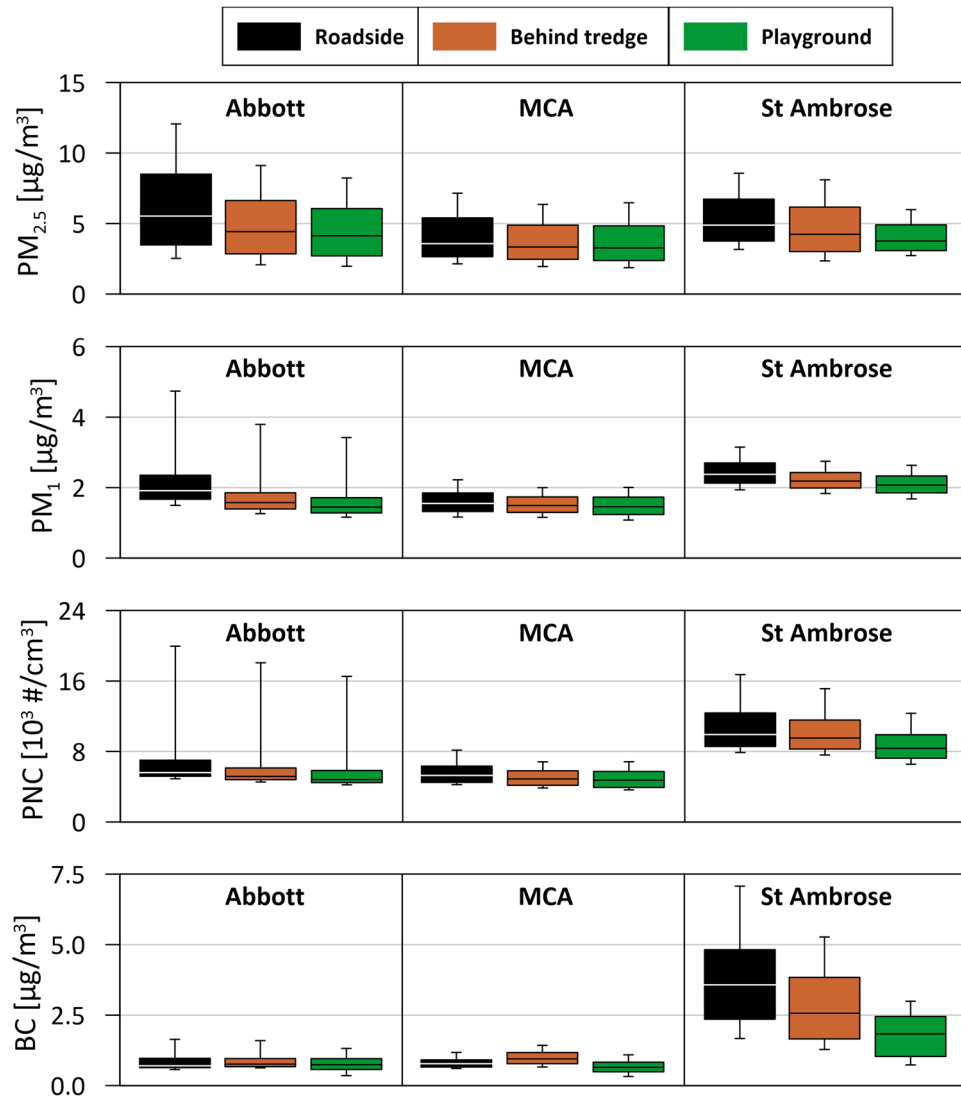


Figure 3. Black carbon (BC), PM_{2.5}, PM₁ and particle number concentrations (PNCs), 1-min aves., measured at the roadsides, and in the playgrounds at 1 m (‘Behind tredege’) and ~5 m (‘Playground’) behind the tredeges. Boxes indicate median value, lower and upper quartiles, and whiskers show 10th and 90th percentiles.

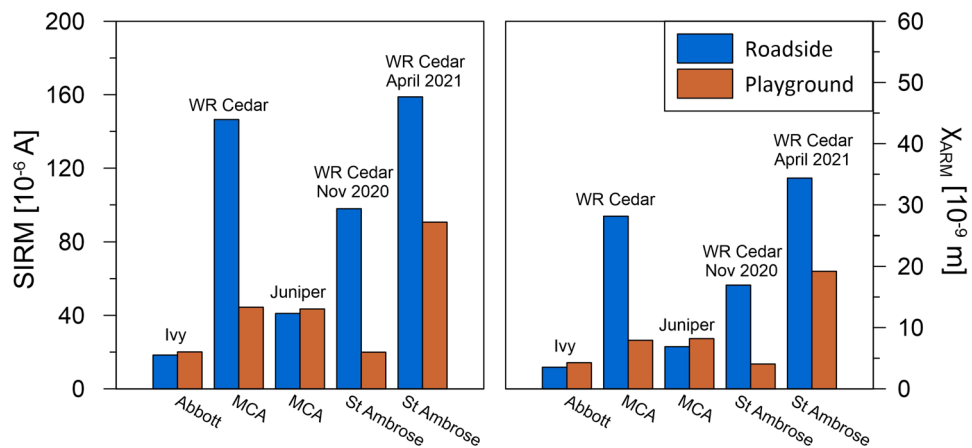


Figure 4. Surface area-specific saturation remanent magnetisation (SIRM) and susceptibility of anhysteretic remanent magnetisation (χ_{ARM}) of leaf samples taken from the roadside and playground sides of the tredeges.

constant, indicating a similar ferrimagnetic grain size population at each site (SI Table S4). Electron microscopy images (e.g., SI Fig. S1) show that the majority of leaf-deposited pollution particles are $< 1 \mu\text{m}$ in size (e.g.^{34,71}).

The leaf magnetic loadings can be used to estimate the total amount of PM_{10} deposited on the leaves and its proportion compared with the total traffic-emitted PM_{10} (SI Table S5). Given, for example, the measured SIRM at St Ambrose ($98\text{--}20 \times 10^{-6}$ A for leaves collected in November 2020), SIRM values for synthetic magnetite of $5.0 \text{ Am}^2/\text{kg}$ (for magnetite grains $0.1\text{--}1 \mu\text{m}$ ⁷²), average mass concentrations of magnetite in roadside dust ($0.32\text{--}0.95$ wt.%; data for a highly-trafficked street in Birmingham, UK³¹), and total leaf surface area ($2.5 \text{ m}^2/\text{tree}$), the estimated leaf PM mass is $\sim 124 \mu\text{g}/\text{cm}^2$ and the total mass of PM_{10} deposited on a tree is $14.7\text{--}22.1 \text{ g}/\text{tree}$. These leaf PM mass estimates are comparable with those measured⁷¹ for four evergreen species, which ranged from $\sim 72 \mu\text{g}/\text{cm}^2$ (in *P. tabulaeformis*) to $232 \mu\text{g}/\text{cm}^2$ (in *J. formosana*). The tregde at St Ambrose comprises 102 western red cedar trees so an estimated $158\text{--}705 \text{ g}$ were deposited on the whole tregde.

For a road section 100 m in length, average traffic count of 80,000 vehicles/day (Fig. 2), and estimated PM_{10} emission factor of $\sim 100 \text{ mg}/(\text{km vehicle})$ ⁵⁶, the average emission mass flow is $\sim 9.3 \text{ mg}/\text{s}$. PM deposition on leaves may reach 'saturation'/equilibrium over ~ 6 dry days³⁵ but PM is washed off leaves during rainfall events. PM wash-off from leaves varies with species, leaf traits and rainfall intensity/duration but removal of $40\text{--}80\%$ of surface-deposited PM has typically been reported for a variety of species (e.g.^{63,73-75}). In November 2020, the tregde leaves were sampled 3 dry days after a rainfall event. Over that time period, therefore, the estimated cumulative traffic-emitted PM_{10} mass is $\sim 2400 \text{ g}$. Assuming the prior rainfall removed either 50% or 75% of the previously-deposited leaf PM, then comparing the PM_{10} mass deposited on the whole tregde (102 western red cedar trees) and the cumulative traffic-emitted PM_{10} mass, we can estimate that between $\sim 7\%$ and 29% of the traffic-emitted PM_{10} was deposited on the western red cedar tregde at St Ambrose at this time (SI Table S5).

Discussion

Given known and suspected impacts of PM exposure on human health, especially for particularly vulnerable population groups (e.g., young children), fast and effective mitigation of exposure levels -even by what is conventionally considered 'small' amounts -is essential. In the UK, COMEAP⁷⁶ estimate that reducing the annual average concentration of $\text{PM}_{2.5}$ by only $1 \mu\text{g}/\text{m}^3$ would save ~ 3.6 million life years, equivalent to an increase in life expectancy of 20 days in people born in 2008.

Here, air quality measurements in open road contexts demonstrate that installation of carefully-selected and designed vegetation structures ('tredges') at the school roadside can rapidly achieve significant reductions in playground PM concentrations. For the ivy screen (Abbott), the measured $\text{PM}_{2.5}$ and PM_1 reductions probably dominantly reflect some blocking of the dominantly westerly airflow and subsequently reduced leeward PM, since PM deposition on the ivy leaves (as measured by leaf magnetic remanences) was low. In contrast, PM deposition on the evergreen western red cedar tregde (St Ambrose) was much greater; leaf magnetic loadings indicate that up to 29% of the local traffic-emitted PM_{10} was deposited on the western red cedar tregde at St Ambrose at the time of sampling (Nov. 2020). It is reasonable to assume that most of the leaf-deposited PM originated from the proximal, traffic-related sources (rather than the regionally-dispersed PM). Since the local, traffic-derived PM increment typically constitutes $\sim 50\%$ of measured ambient PM, then leaf deposition at St Ambrose removed $\sim 46\%$ and 26% of the traffic-sourced $\text{PM}_{2.5}$ and PM_1 , respectively. Further, and possibly of major importance for child health, the tredges substantially reduced the magnitude and frequency of acute 'spikes' in PM and BC concentrations; for example, by $67\text{--}82\%$ for $\text{PM}_{2.5}$, PM_1 and PNC in the St Ambrose playground. The St Ambrose tregde also produced marked reductions in average playground BC concentrations, unlike the other two tredges. Notable is that the playground air quality improvements at St Ambrose were achieved with a narrow ($\sim 1 \text{ m}$) tregde (i.e. 10% of the width recommended by e.g.⁷⁷). This is important; in many urban situations, space for planting roadside tredges is often very limited. The effectiveness of the inner juniper hedge and outer birch/western red cedar tregde (MCA) was less but likely to increase with time (these plants had experienced sparse growth at the times of sampling).

These findings demonstrate that roadside vegetation can be designed, installed and maintained to achieve rapid, significant and cost-effective improvement of air quality by optimising PM deposition on plant leaves. Critical to air quality improvement through PM deposition is selection of species with leaf traits creating high V_d values; combined with high rates of PM removal by rainfall and/or watering wash-off (to restore leaf PM-capturing ability), and permeability (to avoid blocking of PM transport and increased roadside PM). Fowler et al.'s⁶⁴ V_d value of 1.07 cm s^{-1} for urban 'woodland' (mixed oak, sweet chestnut, beech, holly) was described recently as 'high'⁷⁸. Yet, as independently attested by their much higher leaf PM loadings (e.g.,^{61,71}), numerous other species demonstrate higher V_d values (e.g.,³⁵). Hence, substantively higher V_d values need to be included in any modelling study seeking to quantify roadside vegetation and leaf PM deposition effects (e.g.,^{44,57}). The air quality improvements measured here were obtained in open road contexts but it is equally important to incorporate realistic/optimised V_d values in street canyon modelling, to inform any removal of existing (too high/large) vegetation and/or installation of new, optimised vegetation.

To trap PM before its dispersion into the regional airshed, tredges (with near-ground level leaves) should be close to the local, traffic-emitted sources. Tregde height should be managed, around adult head-height and certainly never exceeding the height of any adjacent buildings, to prevent reduced airflow and upward dispersion which large, tall trees can induce, thus worsening roadside pollution⁴⁴. Under dry conditions, watering of tredges might be required, to wash off leaf-accumulated PM into the soil below and renew their leaf PM-capturing capability. Other benefits accrue from roadside greening (e.g., green space wellbeing, noise reduction, visual appeal, safety, privacy, biodiversity benefits, climate change proofing) but species selection must also preclude deleterious effects (e.g., excessive production of allergenic pollen, poisonous fruit/seeds, volatile organic compounds).

Here, the measured amounts of leaf-deposited magnetic PM after tredge installation, and the measured reductions in playground PM, PNC and BC, demonstrate that air quality improvements by deposition can be achieved at the local, near-road, community/playground scale. Modelling/quantification of the complexity of factors (dispersion- and deposition-related) influencing these playground PM concentrations, whilst desirable, would have required substantial additional resources. Beyond this study, and given the importance to human health of immediate exposure reduction, integrated experimental and modelling investigations of roadside greening effects are timely and important. Ideally, robust measurement of species-specific V_d and permeability values under different meteorological and pollution conditions would be combined with iterative modelling of airflow/dispersion and size-specific PM deposition effects. Essential for such investigations are sufficient resource to implement simultaneous, multi-site, robust measurements of PM and PNC (and detailed characterisation of airborne and leaf-deposited PM), combined with sufficient computational resource for model runs incorporating multiple iterations with varying V_d ⁵⁷, rather than/as well as leaf area index and density^{79,80}, permeability and meteorological (especially wind speed) parameterisations. Essential is that vegetation effects are modelled at the micro- as well as the macro-scale⁴⁴.

Finally, if sufficient, well-designed roadside tregdes were installed and managed appropriately along heavily-trafficked streets across an urban area, leading to reduction in the amount of PM leaving those road areas, then PM loadings at the city and regional scale should also fall (albeit with the effect of concentrating pollutants in the soil beneath the tregdes). As an interim, fast and cost-effective measure (i.e., prior to policy-driven reductions of PM emissions), and for protection of brain, heart and pre-natal health, careful use of roadside tregdes should be considered for widespread implementation. City-wide modelling of the air quality impacts of such structures would be of timely value in this context.

Methods

In this study in Manchester, U.K., we investigated the possibility of using optimised green infrastructure -instantly installed 'tregdes'⁽⁵⁸⁾ -to achieve measurable improvements in air quality (PM concentrations) in the playgrounds of four primary schools located adjacent to major arterial routes through the city. These schools are sited within the Greater Manchester Air Quality Management Area (AQMA), where air pollution standards are unlikely to be met.

For air quality monitoring over a period of several months, Cambri sensors (Shenzhen Cambri Environmental Technology Ltd., China) were installed at the roadside and > 10 m from the roadside. Particles with diameters between 0.37 and 17.4 μm were detected using the Alphasense OPC-N2 sensor. The sensors were co-located for cross-calibration of PM_{10} , $\text{PM}_{2.5}$, and PM_1 measurements (via orthogonal regression of data and sensor 1 h or daily means), and estimation of between-sensor uncertainties, before (May 2019) and after (October/November 2019) the monitored interval. A Cambri sensor was also co-located at Manchester University's Air Quality Super Site. The PM data are presented as 1-h average values. For safety reasons, the playground sensors were required to be sited distally (14–17 m) from the road at the rear of the playground areas (for Medlock, St Ambrose and Abbott schools) and close to the school frontage (7 m from the road, MCA school). These locations necessitated use of car batteries to power the sensors; battery failures led to sensor drift and episodic malfunction (creating gaps in data coverage). The PM values recorded by the distal MCA sensor were consistently affected by a nearby air conditioning exhaust outlet.

Black carbon (BC) was measured (MicroAeth M350) simultaneously at roadside and playground, at the 3 schools with tregdes, at morning or evening rush hours in November 2020. Rush hour $\text{PM}_{2.5}$, PM_1 , and PNCs were measured (portable optical particle spectrometers, POPS, Handix Scientific; particle diameter measurement range between ~0.13 to 3.0 μm) simultaneously at roadside and playground at 1 m and ~5 m behind the tregdes in April 2021, after further growth of the tregdes. The POPS and aethalometers were cross-calibrated (co-location at end of the measurement periods), by orthogonal regression of the sensor data vs the sensor mean values (1 min ave.), and uncertainties estimated (<https://ec.europa.eu/environment/air/quality/legislation/pdf/equivalence.pdf>).

Between-sensor uncertainty estimates for the BC measurements range from 2 to 12%, and for the POPS measurements from 1 to 6% (Table S3).

For quantification of magnetic PM loadings, leaves were sampled from the road and playground side of the tregdes and measurements made (at the Centre for Environmental Magnetism & Palaeomagnetism, Lancaster University) of their anhysteretic remanent magnetization (ARM) and saturation remanence (SIRM). ARM is sensitive to the presence of ferrimagnetic particles with a mean particle size of ~25 nm. The SIRM indicates the total concentration of magnetic particles on the leaves. ARM was induced using a Molspin A. F. demagnetiser, with ARM attachment, generating a dc biasing field (0.08 mT) in the presence of an alternating field (100 milliTesla (mT) peak field). The ARM was measured using a spinner magnetometer (JR-6A, AGICO). The susceptibility of ARM (χ_{ARM}) was calculated by normalizing the ARM by the dc biasing field. Room temperature remanent magnetization (SIRM) was acquired in a dc field of 1 T, using a Molspin pulse magnetizer. Calibration of the magnetometer was performed using a cross-calibrated rock sample ($56.05 \times 10^{-8} \text{ Am}^2$). The average value of each magnetic parameter was normalised for the leaf surface area (in m^2). The total leaf surface area was measured for two western red cedar trees, using a Li-Cor Model 3100 area meter, with extrapolation to the installed trees via comparison of their height and trunk diameter at chest height.

Data availability

The published data are available from the corresponding author.

Received: 20 March 2022; Accepted: 9 August 2022

Published online: 20 August 2022

References

- Miller, M. R. & Newby, D. E. Air pollution and cardiovascular disease: Car sick. *Cardiovasc. Res.* **116**, 279–294. <https://doi.org/10.1093/cvr/cvz228> (2019).
- Pope, C. A. III. & Dockery, D. W. Health effects of fine particulate air pollution: Lines that connect. *J. Air Waste Manag. Assoc.* **56**, 709–742 (2006).
- Rajagopalan, S., Al-Kindi, S. G. & Brook, R. D. Air pollution and cardiovascular disease: JACC state-of-the-art review. *J. Am. Coll. Cardiol.* **72**, 2054–2070 (2018).
- Landrigan, P. J. *et al.* The Lancet Commission on pollution and health. *The Lancet* **391**, 462–512 (2018).
- Prüss-Ustün, A. *et al.* Environmental risks and non-communicable diseases. *BMJ* **28**, 364 (2019).
- Kioumourtzoglou, M.-A. *et al.* Long-term PM_{2.5} exposure and neurological hospital admissions in the northeastern United States. *Environ. Health Perspect.* **124**, 23–29 (2016).
- Shi, L. *et al.* Long-term effects of PM_{2.5} on neurological disorders in the American Medicare population: A longitudinal cohort study. *Lancet Planetary Health* **4**, e557–e565 (2020).
- Madureira, J. *et al.* Source apportionment of CO₂, PM₁₀ and VOCs levels and health risk assessment in naturally ventilated primary schools in Porto, Portugal. *Build. Environ.* **96**, 198–205 (2016).
- Maher, B. A., Moore, C. & Matzka, J. Spatial variation in vehicle-derived metal pollution identified by magnetic and elemental analysis of roadside tree leaves. *Atmos. Environ.* **42**, 364–373 (2008).
- Chen, H. *et al.* Living near major roads and the incidence of dementia, Parkinson's disease, and multiple sclerosis: A population-based cohort study. *Lancet* **389**, 718–726 (2017).
- Gauderman, W. J. *et al.* Effect of exposure to traffic on lung development from 10 to 18 years of age: A cohort study. *Lancet* **369**, 571–577 (2007).
- McConnell, R. *et al.* Childhood incident asthma and traffic-related air pollution at home and school. *Environ. Health Perspect.* **118**, 1021–1026 (2010).
- Alvarez-Pedrerol, M. *et al.* Impact of commuting exposure to traffic-related air pollution on cognitive development in children walking to school. *Environ. Pollut.* **231**, 837–844 (2017).
- Amram, O., Abernethy, R., Brauer, M., Davies, H. & Allen, R. W. Proximity of public elementary schools to major roads in Canadian urban areas. *Int. J. Health Geogr.* **10**, 1–11 (2011).
- Kingsley, S. L. *et al.* Proximity of US schools to major roadways: a nationwide assessment. *J. Exposure Sci. Environ. Epidemiol.* **24**, 253–259 (2014).
- Kmietowicz, Z. (British Medical Journal Publishing Group, 2018).
- Sunyer, J. *et al.* Association between traffic-related air pollution in schools and cognitive development in primary school children: A prospective cohort study. *PLoS Med.* **12**, e1001792 (2015).
- Sunyer, J. *et al.* Traffic-related air pollution and attention in primary school children: Short-term association. *Epidemiology* **28**, 181 (2017).
- Lopuszanska, U. & Samardakiewicz, M. The relationship between air pollution and cognitive functions in children and adolescents: A systematic review. *Cogn. Behav. Neurol.* **33**, 157–178 (2020).
- Suglia, S. F., Gryparis, A., Wright, R. O., Schwartz, J. & Wright, R. J. Association of black carbon with cognition among children in a prospective birth cohort study. *Am. J. Epidemiol.* **167**, 280–286. <https://doi.org/10.1093/aje/kwm308> (2008).
- Younan, D. *et al.* Longitudinal analysis of particulate air pollutants and adolescent delinquent behavior in Southern California. *J. Abnorm. Child Psychol.* **46**, 1283–1293 (2018).
- Li, Z. *et al.* Association of ambient air pollutants and birth weight in Ningbo, 2015–2017. *Environ. Pollut.* **249**, 629–637 (2019).
- Stieb, D. M. *et al.* Associations of pregnancy outcomes and PM_{2.5} in a national Canadian study. *Environ. Health Perspect.* **124**, 243–249 (2016).
- Ou, J. Y. *et al.* Fine particulate matter air pollution and mortality among pediatric, adolescent, and young adult cancer patients. *Cancer Epidemiol. Prevent. Biomark.* **29**, 1929–1939 (2020).
- Yuchi, W., Sbihi, H., Davies, H., Tamburic, L. & Brauer, M. Road proximity, air pollution, noise, green space and neurologic disease incidence: A population-based cohort study. *Environ. Health* **19**, 1–15 (2020).
- Power, M. C. *et al.* Traffic-related air pollution and cognitive function in a cohort of older men. *Environ. Health Perspect.* **119**, 682–687 (2011).
- Yang, J. *et al.* Long-term exposure to black carbon and mortality: A 28-year follow-up of the GAZEL cohort. *Environ. Int.* **157**, 106805 (2021).
- Harrison, R. M., Van Vu, T., Jafar, H. & Shi, Z. More mileage in reducing urban air pollution from road traffic. *Environ. Int.* **149**, 106329 (2021).
- Karagulian, F. *et al.* Contributions to cities' ambient particulate matter (PM): A systematic review of local source contributions at global level. *Atmos. Environ.* **120**, 475–483 (2015).
- Sanderson, P., Delgado-Saborit, J. M. & Harrison, R. M. A review of chemical and physical characterisation of atmospheric metallic nanoparticles. *Atmos. Environ.* **94**, 353–365 (2014).
- Gonet, T., Maher, B. A. & Kukutschová, J. Source apportionment of magnetite particles in roadside airborne particulate matter. *Sci. Total Environ.* **752**, 141828. <https://doi.org/10.1016/j.scitotenv.2020.141828> (2021).
- Gonet, T. *et al.* Size-resolved, quantitative evaluation of the magnetic mineralogy of airborne brake-wear particulate emissions. *Environ. Pollut.* **288**, 117808 (2021).
- Kukutschová, J. *et al.* On airborne nano/micro-sized wear particles released from low-metallic automotive brakes. *Environ. Pollut.* **159**, 998–1006 (2011).
- Mitchell, R. & Maher, B. A. Evaluation and application of biomagnetic monitoring of traffic-derived particulate pollution. *Atmos. Environ.* **43**, 2095–2103 (2009).
- Mitchell, R., Maher, B. A. & Kinnersley, R. Rates of particulate pollution deposition onto leaf surfaces: Temporal and inter-species magnetic analyses. *Environ. Pollut.* **158**, 1472–1478. <https://doi.org/10.1016/j.envpol.2009.12.029> (2010).
- Sagnotti, L., Macri, P., Egli, R. & Mondino, M. Magnetic properties of atmospheric particulate matter from automatic air sampler stations in Latium (Italy): Toward a definition of magnetic fingerprints for natural and anthropogenic PM₁₀ sources. *J. Geophys. Res. Solid Earth* **111**, B12 (2006).
- Frye, C. *et al.* Association of lung function with declining ambient air pollution. *Environ. Health Perspect.* **111**, 383–387 (2003).
- Avol, E. L., Gauderman, W. J., Tan, S. M., London, S. J. & Peters, J. M. Respiratory effects of relocating to areas of differing air pollution levels. *Am. J. Respir. Crit. Care Med.* **164**, 2067–2072 (2001).
- Abhijith, K. V. *et al.* Air pollution abatement performances of green infrastructure in open road and built-up street canyon environments—A review. *Atmos. Environ.* **162**, 71–86. <https://doi.org/10.1016/j.atmosenv.2017.05.014> (2017).
- Al-Dabbous, A. N. & Kumar, P. The influence of roadside vegetation barriers on airborne nanoparticles and pedestrians exposure under varying wind conditions. *Atmos. Environ.* **90**, 113–124. <https://doi.org/10.1016/j.atmosenv.2014.03.040> (2014).

41. Maher, B. A., Ahmed, I. A. M., Davison, B., Karloukovski, V. & Clarke, R. Impact of roadside tree lines on indoor concentrations of traffic-derived particulate matter. *Environ. Sci. Technol.* **47**, 13737–13744. <https://doi.org/10.1021/es404363m> (2013).
42. Tomson, M. *et al.* Green infrastructure for air quality improvement in street canyons. *Environ. Int.* **146**, 106288. <https://doi.org/10.1016/j.envint.2020.106288> (2021).
43. McDonald, R., Kroeger, T., Boucher, T., Wang, L., & Salem, R. *Planting Healthy Air: A Global Analysis of the Role of Urban Trees in Addressing Particulate Matter Pollution and Extreme Heat*. Vol. 136. (2016).
44. Santiago, J.-L., Martilli, A. & Martin, F. On dry deposition modelling of atmospheric pollutants on vegetation at the microscale: Application to the impact of street vegetation on air quality. *Bound.-Layer Meteorol.* **162**, 451–474. <https://doi.org/10.1007/s10546-016-0210-5> (2017).
45. Group, A. Q. E. (ed. Food and Rural Affairs; Scottish Government; Welsh Government; and Department of the Environment in Northern Ireland. Prepared for the Department for Environment) (2018).
46. Pearce, H., Levine, J. G., Cai, X. & MacKenzie, A. R. Introducing the green infrastructure for roadside air quality (GI4RAQ) platform: Estimating site-specific changes in the dispersion of vehicular pollution close to source. *Forests* <https://doi.org/10.3390/f12060769> (2021).
47. Jeanjean, A. P. R., Buccolieri, R., Eddy, J., Monks, P. S. & Leigh, R. J. Air quality affected by trees in real street canyons: The case of Marylebone neighbourhood in central London. *Urban For. Urban Green.* **22**, 41–53. <https://doi.org/10.1016/j.ufug.2017.01.009> (2017).
48. Jeanjean, A. P. R., Monks, P. S. & Leigh, R. J. Modelling the effectiveness of urban trees and grass on PM_{2.5} reduction via dispersion and deposition at a city scale. *Atmos. Environ.* **147**, 1–10. <https://doi.org/10.1016/j.atmosenv.2016.09.033> (2016).
49. Nowak, D. J., Crane, D. E. & Stevens, J. C. Air pollution removal by urban trees and shrubs in the United States. *Urban For. Urban Green.* **4**, 115–123. <https://doi.org/10.1016/j.ufug.2006.01.007> (2006).
50. Vos, P. E. J., Maiheu, B., Vankerkom, J. & Janssen, S. Improving local air quality in cities: To tree or not to tree?. *Environ. Pollut.* **183**, 113–122. <https://doi.org/10.1016/j.envpol.2012.10.021> (2013).
51. Beckett, K. P., Freer-Smith, P. H. & Taylor, G. Particulate pollution capture by urban trees: effect of species and windspeed. *Glob. Change Biol.* **6**, 995–1003 (2000).
52. Freer-Smith, P. H., Beckett, K. P. & Taylor, G. Deposition velocities to *Sorbus aria*, *Acer campestre*, *Populus deltoides* × *trichocarpa* 'Beaupré', *Pinus nigra* and × *Cupressocyparis leylandii* for coarse, fine and ultra-fine particles in the urban environment. *Environ. Pollut.* **133**, 157–167. <https://doi.org/10.1016/j.envpol.2004.03.031> (2005).
53. Gallagher, M. W. *et al.* Measurements of aerosol fluxes to speulder forest using a micrometeorological technique. *Atmos. Environ.* **31**, 359–373. [https://doi.org/10.1016/S1352-2310\(96\)00057-X](https://doi.org/10.1016/S1352-2310(96)00057-X) (1997).
54. Janhäll, S. Review on urban vegetation and particle air pollution—Deposition and dispersion. *Atmos. Environ.* **105**, 130–137. <https://doi.org/10.1016/j.atmosenv.2015.01.052> (2015).
55. Zhang, L., Gong, S., Padro, J. & Barrie, L. A size-segregated particle dry deposition scheme for an atmospheric aerosol module. *Atmos. Environ.* **35**, 549–560. [https://doi.org/10.1016/S1352-2310\(00\)00326-5](https://doi.org/10.1016/S1352-2310(00)00326-5) (2001).
56. Litschke, T. & Kuttler, W. On the reduction of urban particle concentration by vegetation—A review. *Meteorol. Z.* **17**, 229–240 (2008).
57. Santiago, J.-L. *et al.* CFD modelling of vegetation barrier effects on the reduction of traffic-related pollutant concentration in an avenue of Pamplona, Spain. *Sustain. Cities Soc.* **48**, 101559. <https://doi.org/10.1016/j.scs.2019.101559> (2019).
58. Wang, H., Maher, B. A., Ahmed, I. A. M. & Davison, B. Efficient removal of ultrafine particles from diesel exhaust by selected tree species: Implications for roadside planting for improving the quality of urban air. *Environ. Sci. Technol.* **53**, 6906–6916. <https://doi.org/10.1021/acs.est.8b06629> (2019).
59. Pugh, T. A. M., MacKenzie, A. R., Whyatt, J. D. & Hewitt, C. N. Effectiveness of green infrastructure for improvement of air quality in urban street canyons. *Environ. Sci. Technol.* **46**, 7692–7699. <https://doi.org/10.1021/es300826w> (2012).
60. Muhammad, S., Wuyts, K. & Samson, R. Species-specific dynamics in magnetic PM accumulation and immobilization for six deciduous and evergreen broadleaves. *Atmos. Pollut. Res.* **13**, 101377. <https://doi.org/10.1016/j.apr.2022.101377> (2022).
61. Sæbø, A. *et al.* Plant species differences in particulate matter accumulation on leaf surfaces. *Sci. Total Environ.* **427–428**, 347–354. <https://doi.org/10.1016/j.scitotenv.2012.03.084> (2012).
62. Weber, F., Kowarik, I. & Säumlé, I. Herbaceous plants as filters: Immobilization of particulates along urban street corridors. *Environ. Pollut.* **186**, 234–240. <https://doi.org/10.1016/j.envpol.2013.12.011> (2014).
63. Chen, L., Liu, C., Zhang, L., Zou, R. & Zhang, Z. Variation in tree species ability to capture and retain airborne fine particulate matter (PM_{2.5}). *Sci. Rep.* **7**, 3206. <https://doi.org/10.1038/s41598-017-03360-1> (2017).
64. Fowler, D. S. U. *et al.* Measuring aerosol and heavy metal deposition on urban woodland and grass using inventories of 210Pb and metal concentrations in soil. *Water Air Soil Pollut. Focus* **4**, 483–499 (2004).
65. Quarg Harrison, R. M., Brimblecombe, P., Derwent, R. G., Dollard, G. J., Eggleston, S., Hamilton, R. S. & Moorcroft, S. (ed. Third report to the Department of the Environment; Quality of Urban Air Review Group (QUARG)) (HMSO, 1996).
66. Abhijith, K. V. & Kumar, P. Field investigations for evaluating green infrastructure effects on air quality in open-road conditions. *Atmos. Environ.* **201**, 132–147. <https://doi.org/10.1016/j.atmosenv.2018.12.036> (2019).
67. Winkler, A. *et al.* Magnetic emissions from brake wear are the major source of airborne particulate matter bioaccumulated by Lichens exposed in Milan (Italy). *Appl. Sci.* <https://doi.org/10.3390/app10062073> (2020).
68. Matzka, J. & Maher, B. A. Magnetic biomonitoring of roadside tree leaves: Identification of spatial and temporal variations in vehicle-derived particulates. *Atmos. Environ.* **33**, 4565–4569. [https://doi.org/10.1016/S1352-2310\(99\)00229-0](https://doi.org/10.1016/S1352-2310(99)00229-0) (1999).
69. Kończak, B., Cempa, M., Pierzchała, Ł. & Deska, M. Assessment of the ability of roadside vegetation to remove particulate matter from the urban air. *Environ. Pollut.* **268**, 115465. <https://doi.org/10.1016/j.envpol.2020.115465> (2021).
70. Przybysz, A., Sæbø, A., Hanslin, H. M. & Gawroński, S. W. Accumulation of particulate matter and trace elements on vegetation as affected by pollution level, rainfall and the passage of time. *Sci. Total Environ.* **481**, 360–369. <https://doi.org/10.1016/j.scitotenv.2014.02.072> (2014).
71. Song, Y. *et al.* Particulate matter deposited on leaf of five evergreen species in Beijing, China: Source identification and size distribution. *Atmos. Environ.* **105**, 53–60. <https://doi.org/10.1016/j.atmosenv.2015.01.032> (2015).
72. Maher, B. A. Magnetic properties of some synthetic sub-micron magnetites. *Geophys. J. Int.* **94**, 83–96. <https://doi.org/10.1111/j.1365-246X.1988.tb03429.x> (1988).
73. Popek, R., Łukowski, A., Bates, C. & Oleksyn, J. Accumulation of particulate matter, heavy metals, and polycyclic aromatic hydrocarbons on the leaves of *Tilia cordata* Mill. in five Polish cities with different levels of air pollution. *Int. J. Phytoremediat.* **19**, 1134–1141. <https://doi.org/10.1080/15226514.2017.1328394> (2017).
74. Xu, X. *et al.* Influence of rainfall duration and intensity on particulate matter removal from plant leaves. *Sci. Total Environ.* **609**, 11–16. <https://doi.org/10.1016/j.scitotenv.2017.07.141> (2017).
75. Muhammad, S., Wuyts, K. & Samson, R. Atmospheric net particle accumulation on 96 plant species with contrasting morphological and anatomical leaf characteristics in a common garden experiment. *Atmos. Environ.* **202**, 328–344 (2019).
76. Pollutants, C. o. t. M. E. o. A. (ed. Department of Health) (Department of Health, 2010).
77. Baldauf, R. Roadside vegetation design characteristics that can improve local, near-road air quality. *Transp. Res. Part D Transp. Environ.* **52**, 354–361. <https://doi.org/10.1016/j.trd.2017.03.013> (2017).

78. Hewitt, C. N., Ashworth, K. & MacKenzie, A. R. Using green infrastructure to improve urban air quality (GI4AQ). *Ambio* **49**, 62–73. <https://doi.org/10.1007/s13280-019-01164-3> (2020).
79. Steffens, J. T., Wang, Y. J. & Zhang, K. M. Exploration of effects of a vegetation barrier on particle size distributions in a near-road environment. *Atmos. Environ.* **50**, 120–128. <https://doi.org/10.1016/j.atmosenv.2011.12.051> (2012).
80. Tong, Z., Baldauf, R. W., Isakov, V., Deshmukh, P. & Max Zhang, K. Roadside vegetation barrier designs to mitigate near-road air pollution impacts. *Sci. Total Environ.* **541**, 920–927. <https://doi.org/10.1016/j.scitotenv.2015.09.067> (2016).

Acknowledgements

We acknowledge the support of Manchester City Council and Transport for Greater Manchester in funding this study, and Groundwork UK who collaborated in achieving project funding and installed the treads. The University of Manchester Air Quality Supersite was funded through NERC Capital Investment and its running costs are currently supported through the UKRI Clean Air programme grant. Intercomparison infrastructure at the supersite was funded by OSCA (NE/T001984/1).

Author contributions

B.A.M. conceived the study, carried out field measurements, analysed the data, and wrote, reviewed and edited the paper. T.G. analysed the data, and contributed to writing and editing the paper. V.V.K. carried out field measurements and commented on the paper. W.H. carried out field measurements, analysed the data and commented on the paper. T.B. contributed to the data curation and formal analysis and commented on the paper.

Competing interests

The authors declare no competing interests.

Additional information

Supplementary Information The online version contains supplementary material available at <https://doi.org/10.1038/s41598-022-18509-w>.

Correspondence and requests for materials should be addressed to B.A.M.

Reprints and permissions information is available at www.nature.com/reprints.

Publisher's note Springer Nature remains neutral with regard to jurisdictional claims in published maps and institutional affiliations.



Open Access This article is licensed under a Creative Commons Attribution 4.0 International License, which permits use, sharing, adaptation, distribution and reproduction in any medium or format, as long as you give appropriate credit to the original author(s) and the source, provide a link to the Creative Commons licence, and indicate if changes were made. The images or other third party material in this article are included in the article's Creative Commons licence, unless indicated otherwise in a credit line to the material. If material is not included in the article's Creative Commons licence and your intended use is not permitted by statutory regulation or exceeds the permitted use, you will need to obtain permission directly from the copyright holder. To view a copy of this licence, visit <http://creativecommons.org/licenses/by/4.0/>.

© The Author(s) 2022